JOC The Journal of Organic Chemistry

Article

[a]-Phenanthrene-Fused BF2 Azadipyrromethene (azaBODIPY) Dyes as Bright Near-Infrared Fluorophores

Wanle Sheng, Jiuen Cui, Zheng Ruan, Lifeng Yan, Qinghua Wu, Changjiang Yu, Yun Wei, Erhong Hao, and Lijuan Jiao

J. Org. Chem., **Just Accepted Manuscript** • DOI: 10.1021/acs.joc.7b01803 • Publication Date (Web): 13 Sep 2017

[*a*]-Phenanthrene-Fused BF_2 Azadipyrromethene (azaBODIPY) Dyes as Bright Near-Infrared Fluorophores

Wanle Sheng,[†] *Jiuen Cui,*[†] *Zheng Ruan,*[‡] *Lifeng Yan,*[‡] *Qinghua Wu,*[†] *Changjiang Yu,*[†] *Yun Wei,*[†] *Erhong Hao**[†] *and Lijuan Jiao**[†]

[†]Laboratory of Functional Molecular Solids, Ministry of Education; Anhui Laboratory of Molecule-Based Materials (State Key Laboratory Cultivation Base) and School of Chemistry and Materials Science, Anhui Normal University, No.1 East Beijing Road, Wuhu, 241000, China.

[‡]CAS Key Laboratory of Soft Matter Chemistry, Hefei National Laboratory for Physical Sciences at the Microscale, iChEM, and Department of Chemical Physics, University of Science and Technology of China, Jinzai Road 96#, Hefei, 230026 Anhui, China.

*To whom correspondence should be addressed.

E-mail: haoehong@ahnu.edu.cn, jiao421@ahnu.edu.cn

Abstract Graphic

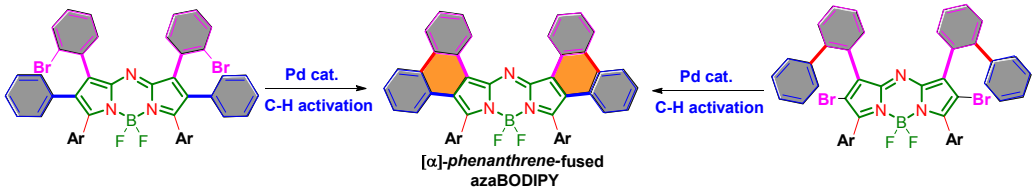

Abstract: A new substitution pattern of BF_2 azadipyrromethene (azaBODIPY) dyes was obtained by phenanthrene fusion through a key palladium-catalyzed intramolecular C-H activation reaction. These [*a*]-phenanthrene-fused azaBODIPYs have near planar structure of the phenanthrene-fused azadipyrromethene core in the crystalline state. The chromophore absorbs (log ε > 5) and fluoresces (ϕ = 0.32-0.38) strongly above 700 nm with excellent photostability, and may be used as an attractive bright NIR bioimaging agent.

INTRODUCTION

New design strategies for functional organic chromophores, especially those absorbing and/or emitting in the near-infrared (NIR) spectroscopic window (700-1000 nm) are of great interest for the continuous development of high-contrast bio-imaging agent, optical recording material, NIR laser filter, photographic material and photosensitizers for solar cells.[1] BF_2 azadipyrromethenes (azaBODIPYs) firstly reported by O'Shea et al.[2-4] have received extensive research interests due to their remarkable photophysical properties, such as the inherent strong long wavelength absorption (around 650 nm) and easy accessibility. Several elegant researches have been performed to further red shift their absorption and emission bands to NIR regions, including the installation of electron-donating and/or electron-withdrawing substituents to the parent π–conjugated framework (*via* "push-pull" effect),[5,6] and the installation of six member ring(s) to rigidify 3,5-aryls (*via* "conformational-restriction" strategy, Chart S1 in the supporting information)[7,8].

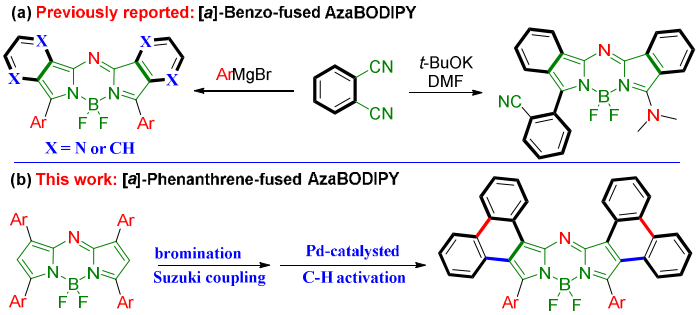

Figure 1. Reported synthesis of [*a*]-benzo-fused azaBODIPYs[13-14] (a) and the synthetic strategies for [*a*]-phenanthrene-fused azaBODIPYs in this work (b).

On the other hand, direct annulations of azaBODIPYs with aromatic rings at the peripheral positions of the chromophore bring the desired structure rigidity and NIR

absorption.[9-11] The recently reported benzo/pyrazine-fused azaBODIPYs[9] and lately disclosed unsymmetrical benzo-fused azaBODIPYs by Shen and coworkers[10] using phthalonitrile as the starting material (Figure 1a) are the only examples to achieve [*a*]-ring-fused azaBODIPYs.

Recently, we reported [*b*]-bisphenanthrene-fused azaBODIPYs from a key intramolecular oxidative aromatic coupling reaction mediated by iron(III) chloride.[12] These [*b*]-bisphenanthrene-fused azaBODIPYs showed decreased fluorescence and interesting semiconducting properties. Herein, we report a novel method to synthesize three [*a*]-phenanthrene-fused azaBODIPYs (Figure 1b) *via* the bromination, Suzuki coupling in concert with the key palladium-catalyzed intramolecular C-H activation reaction.[13] The X-ray structures, electronic and optical properties of these resultant dyes were investigated and compared with corresponding [*b*]-bisphenanthrene-fused azaBODIPYs .

RESULTS AND DISCUSSION

Syntheses

The starting azaBODIPY **1** was prepared in 35% overall yield over three steps from commercially available 4-methoxyacetophenone and 3,4,5-trimethoxybenzaldehyde (Scheme S1 in the supporting information). Bromination of **1** with 2.3 equiv. of liquid bromine afforded 2,6-dibromoazaBODIPY **1Br** in 78% yield. Subsequent Suzuki coupling on **1Br** with 4-*tert*-butylphenylboronic acid provided hexaphenylazaBODIPY **2** in 75% yield (Scheme 1). We rationalized that the installation of the three methoxy directing groups on 1,7-phenyls of azaBODIPY **2** would be able to activate this site to participate in the oxidative-ring-closure reaction to achieve [*a*]-phenanthrene-fused azaBODIPY **4a**. Interestingly, the application of **2**

for the oxidative-ring-fusion reaction with 10 equiv. of $FeCl_3$ in CH_2Cl_2/CH_3NO_2 at room temperature still generated exclusively [*b*]-annulated **3** as a slightly polar product in 87% yield (Scheme 1). Similar to previous report,[12] azaBODIPY **3** showed a 103 nm red-shift in the absorption (centered at 797 nm) with respect to **2** (centered at 694 nm) in toluene. This indicates the successive ring fusion on the chromophore. HRMS (APCI) showed a parent ion peak at m/z 998.4348 (calcd. for $C_{60}H_{59}O_8N_3BF_2$ $[M+H]^+$ 998.4358) for this compound, indicating that only four protons have been removed from this reaction. This loss of four protons was further confirmed by ^1H NMR spectra.

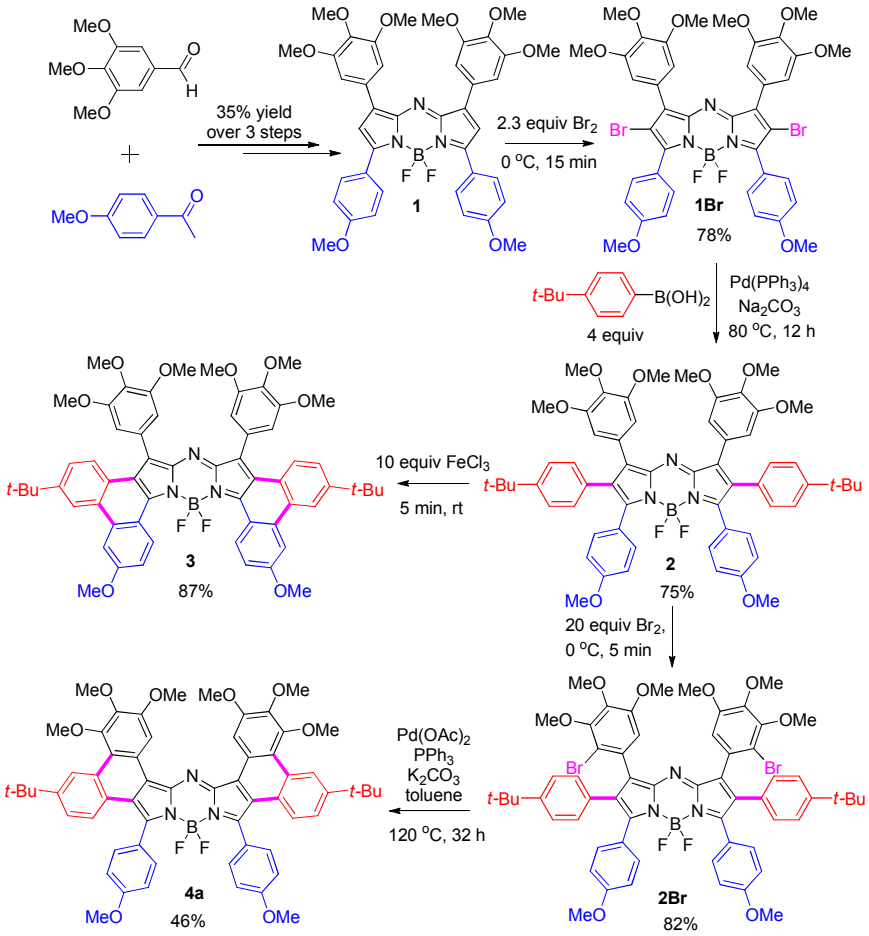

Scheme 1. Synthesis of [*a*]-phenanthrene-fused azaBODIPYs **3** and **4a**.

We thus turned to develop a new method for regioselective synthesis of [*a*]-fused

azaBODIPY **4a** (Scheme 1) through an intramolecular C-H activation reaction of azaBODIPY **2Br**, in which Br groups were installed on 2 positions of 1,7-phenyl groups. By taking advantage of the three electron-rich directing methoxy groups on the 1,7-phenyls of azaBODIPY **2**, dibromohexaphenylazaBODIPY **2Br** was obtained regioselectively in 82% yield from the bromination of hexaphenylazaBODIPY **2** with 20 equiv. of liquid bromine. [*a*]-Annulated isomer **4a** was successfully synthesized in 46% yield from dibromohexaphenylazaBODIPY **2Br** through intramolecular C-H activation reaction using $Pd(OAc)_2$ as catalyst under anhydrous air-free conditions (Scheme 1). The formation of **4a** was confirmed by ^{1}H and ^{13}C NMR and HRMS with a parent ion peak at *m/z* 998.4350 (calcd. for $C_{60}H_{59}O_8N_3BF_2$ *m/z* 998.4358 $[M+H]^+$). Compound **4a** showed a 51 nm red-shift in the absorption (centered at 745 nm) with respect to **2** (centered at 694 nm) in toluene. Fortunately, the [*a*]-phenanthrene-fused azaBODIPY **4a** was unambiguously confirmed via the X-ray crystallographic analysis (Figure 2d).

With the successful syntheses of [*a*]-phenanthrene-fused azaBODIPY **4a**, we next attempted to further apply the above developed method to synthesize [*a*]-phenanthrene-fused **4b**. 3,5-Di-(4-methoxyphenyl)-1,7-di-(2-bromopheny)azaBODIPY **5**, as the key precursor for [*a*]-phenanthro-azaBODIPYs was generated in 30% overall yield in three steps (Scheme S2 in the supporting information) from commercially available 2-bromobenzaldehyde and 4-methoxyacetophenone. AzaBODIPY **6** was then synthesized from the Suzuki reaction between 4-*tert*-butylbenzeneboronic acid and **5** in 92% yield (Scheme 2). The oxidative ring-fusion reaction of **6** under $FeCl_3$ in CH_2Cl_2 and other conditions was failed, probably due to the poor stability of target [*a*]-phenanthrene-fused **4b** under the reaction condition. Thus, treatment of **6** with

liquid bromine afforded the **6Br** in 72% yield. The palladium catalyzed intramolecular C-H activation of **6Br** successfully gave the mixture of [*a*]-phenanthrene-fused azaBODIPYs **4b** and **4c** in 27% and 38% yields, respectively (Scheme 2). All these resulting azaBODIPYs were characterized by NMR and HRMS, and [*a*]-phenanthrene-fused azaBODIPY **4c** was further characterized by X-ray crystallographic analysis (Figure 2c).

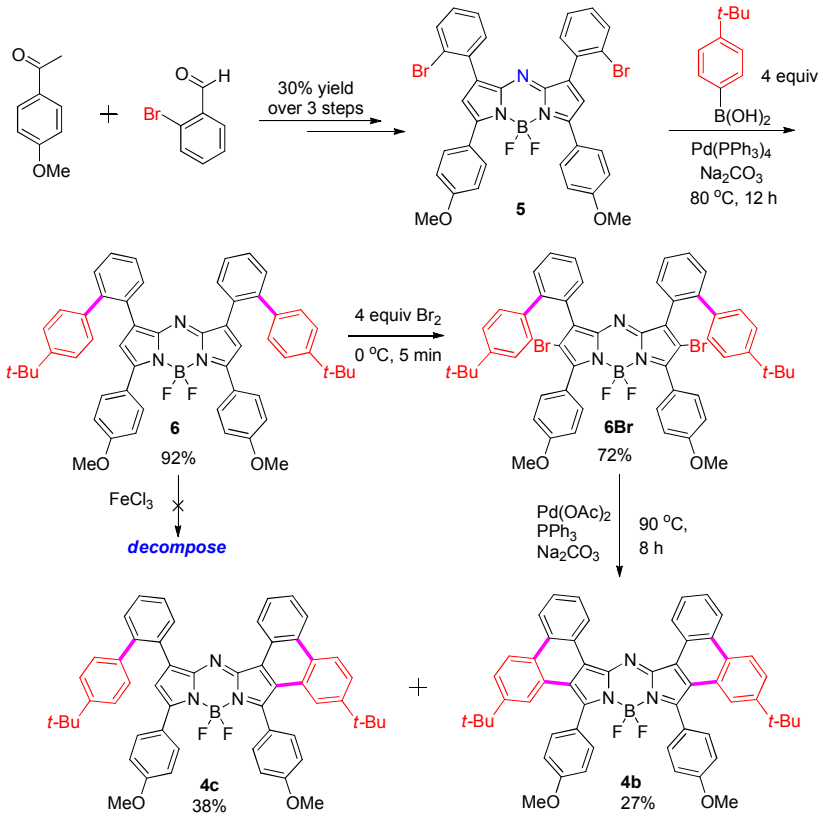

Scheme 2. Synthesis of [*a*]-phenanthrene-fused azaBODIPYs **4b** and **4c**.

X-ray Structure

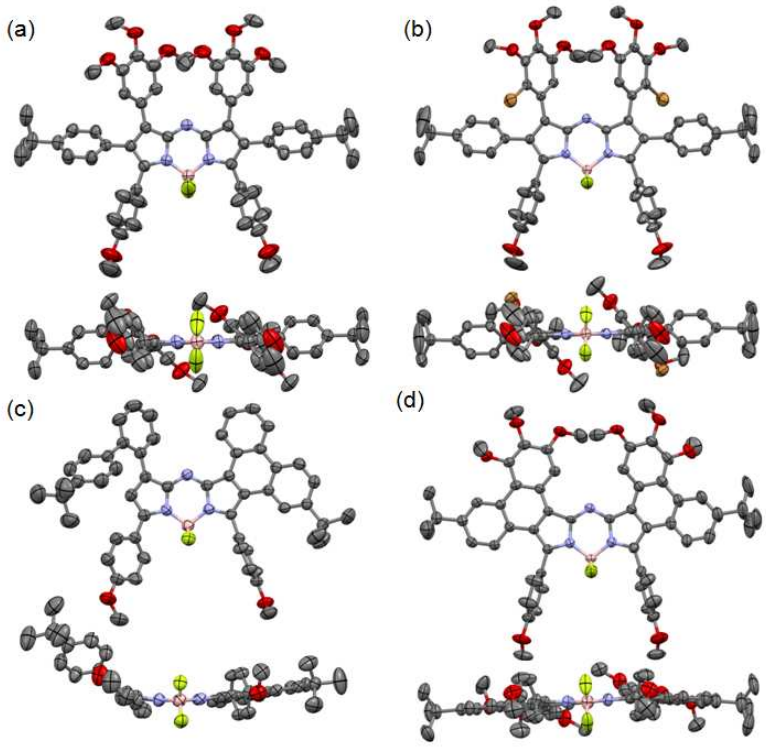

Figure 2. Top (and side) views of the X-ray crystal structures of (a) **2**, (b) **2Br**, (c) **4c** and (d) **4a**. Thermal ellipsoids were shown at 50 % probability. The gray-, blue-, red-, pink-, olivine and orange-colored atoms represent C, N, O, B, F and Br, respectively. Hydrogen atoms are omitted for clarity.

Crystals of **2**, **2Br**, **4a** and **4c** suitable for X-ray analysis were obtained from the slow diffusion of anhydrous ethanol or hexane into their dichloromethane solutions (within one week) at room temperature. These azaBODIPYs showed small pyrrole-pyrrole dihedral angle (<7.1°, Table S1 in the supporting information), with typical B-N and B-F bond lengths (1.54-1.57 Å and 1.35-1.39 Å, respectively, Table S2). AzaBODIPY **4a** showed a small phenanthrene-phenanthrene dihedral angle (8.37^{o}). The bond lengths of C-C, pyrrolic and nonpyrrolic C-N within the azadipyrromethene framework of **4a** showed no clear distinction between the single and double bonds (Table S2 in the supporting information). Thus, the annulations of

phenanthrene moieties to the azaBODIPY core cause little structural disruption of the planarity of the core structure. On the other hand, it greatly affected the dihedral angles between the azadipyrromethene framework and the aryl substituents (*Pa*-*Pc*) (Table S3 in the supporting information). For example, the dihedral angles between azadipyrromethene framework and 1,7/2,6-phenyls (*Pa* and *Pc*) are between 45-54° for **2** and **2Br**, respectively. These dihedral angles were significantly decreased to less than 16° in **4a**. By contrast, a gradually increased dihedral angle between 3,5-phenyls (*Pb*) and the azadipyrromethene framework was observed for **4a** (78°) with respect to **2** and **2Br** (61 and 65°, respectively). Similar trends were clearly observed in the unsymmetrical azaBODIPY **4c** (Table S4 in the supporting information), in which the dihedral angles between azadipyrromethene framework and 1,7- or 3,5-phenyls are 3.5° (*Pa)*, 34° (*Pa*'), 33° (*Pb*) and 86° (*Pb*'), respectively.

Spectroscopic properties

The absorption spectra of **3** and **4a** in toluene were compared with the parent **2** to evaluate the impact of different fusion positions on extending the conjugation of the system (Figure 3a and Table 1). AzaBODIPYs **3** and **4a** each showed a typical narrow absorption band similar to most azaBODIPYs, with the absorption maximum centered at 797 and 745 nm, respectively. The larger red-shifted absorption was observed for **3** over **4a** (103 and 51 nm, respectively) with respect to **2**, indicating [*b*]-fusion may be more efficient in extending the π-conjugation and reducing the HOMO-LUMO gap.[14a] In addition, [*b*]-fusion doubled the molar absorptivity (ε = 162700 $M^{-1}cm^{-1}$ for **3**) with respect to **2** (ε = 79500 $M^{-1}cm^{-1}$), while a smaller enhancement was observed for [*a*]-isomer **4a** (ε = 124700 $M^{-1}cm^{-1}$).

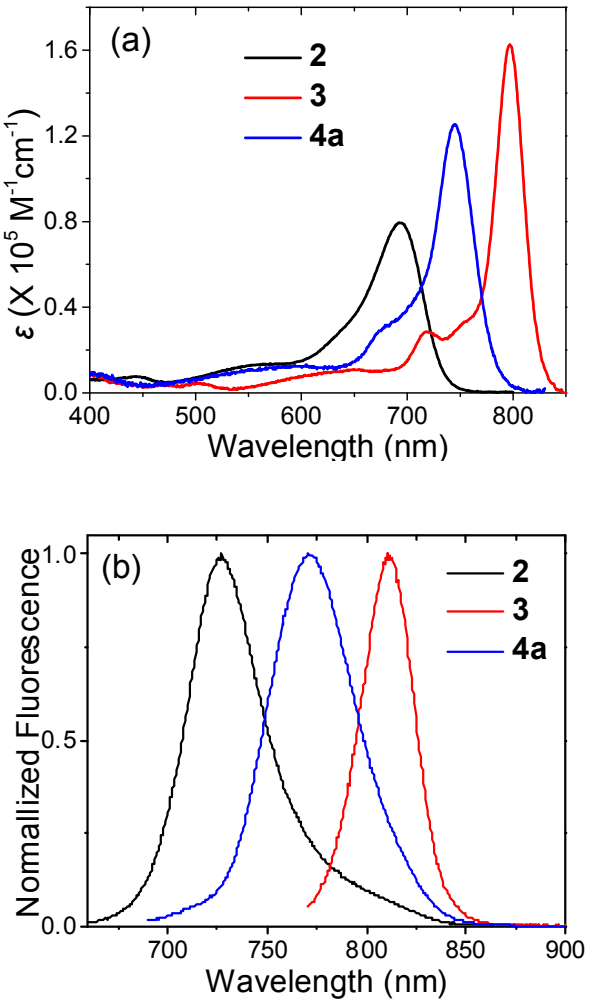

Figure 3. Overlaid absorption (a) and normalized fluorescence emission (b) spectra of **2**, **3** and **4a** in toluene.

Similar modulations in the fluorescence behaviour were also observed with the variation of the fusion positions (Figure 3b). A 45 and 84 nm red-shifted fluorescence emission was observed for **3** and **4a** (λ_{em}^{max} = 810 and 771 nm, respectively) with respect to **2**, respectively. Interestingly, [*a*]-annulated **4a** showed intense fluorescence (ϕ = 0.35) in toluene, while its isomer **3** showed very weak fluorescence emission comparable to that of parent **2**.[14] The origin of the weak fluorescence for **2** may associated with the internal conversion due to the rotation of six aryl groups. This

remarkablely intense fluorescence was also observed for [*a*]-phenanthrene-fused azaBODIPYs **4b** and **4c**. **4b** and **4c** showed emission maxima at 741 and 723 nm with fluorescent quantum yields of 0.32 and 0.38, respectively. More importantly, both annulated dyes **3** and **4a** showed comparably good photostabilities with that of parent 1,3,5,7-tetraphenylaza-BODIPY in toluene (Figure S15 in the supporting information).

Table 1. Photophysical properties of azaBODIPYs **1-4** at room temperature in toluene.

dyes	λ_{abs}^{max} (nm)	λ_{em}^{max} (nm)	ε (M^{-1} cm^{-1})	Φ [a]	Stokes-shift (cm^{-1})
1	698	724	91900	0.24	514
1Br	689	723	72700	0.002	683
2	694	726	79500	0.04	635
2Br	706	740	65800	0.08	651
3	797	810	162700	0.05	201
4a	745	771	124700	0.35	453
4b	716	741	147700	0.32	471
4c	701	723	100400	0.38	434

[a]fluorescence quantum yields were obtained by using 1,7-diphenyl-3,5-dimehoxyphenyl-azadipyrromethene (Φ = 0.36 in chloroform) as reference compound for **1**, **1Br**, **2**, **2Br**, **4b**, **4c** and Indocyanine Green (ICG) (ϕ = 0.12 in DMSO) for **3** and **4a**. The standard errors are less than 10%.

DFT calculations

To elucidate the influence of fusion positions on the electronic and optical properties of these phenanthrene-annulated azaBODIPYs, cyclic voltammetry of these dyes was studied (Figure S16 and Table S5 in the supporting information). AzaBODIPYs **1**-**4** each displayed a reversible or quasi-reversible reduction wave, with a reversible or quasi-reversible oxidation wave. [*a*]-Annulation in **4a** mainly increased the HOMO energy level to -5.28 eV from -5.40 eV for **2**, which were calculated from their onset potential of the first oxidation and reduction waves. This result is similar to most reported aromatic-ring annulated chromophores[9,11], in which the decrease of bandgaps were generally achieved *via* the increase of HOMO energy levels. By contrast, the overall decreased bandgap observed for [*b*]-annulated **3** (relative to **4a**) not only came from the increased HOMO energy level to -5.29 eV from -5.40 eV for **2**, but also came from the decreased LUMO energy level to -4.07 eV from -3.91 eV for **2**. The HOMO-LUMO energy gap of **3** is smaller than that of **4a**, which is in good agreement with the absorption spectra shown in Figure 3a.

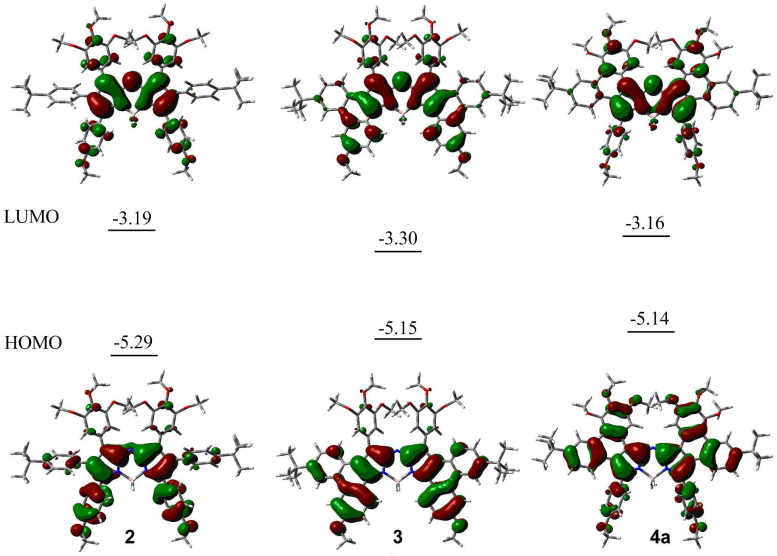

Figure 4. Frontier molecular orbitals and the energies of **2, 3** and **4a**.

DFT calculations indicate that the HOMO orbitals are mainly delocalized over both the central azadipyrromethene framework and the phenanthrene moieties for both **3** and **4a**, while the HOMO coefficients are mainly located on the central azadipyrromethene framework and 3,5- phenyls for **2** (Figure 4). The LUMO coefficients are mainly located on the central azadipyrromethene framework and 3,5-phenyls for both **2** and [*b*]-annulated **3**, while, in contrast, the LUMO orbitals are mainly located on the central azadipyrromethene framework and 1,7- phenyls for [*b*]-annulated **4a** (Figure 4). In comparison with **2**, both annulated isomers showed destabilized calculated HOMO energy levels, while only [*b*]-isomer also showed stabilized LUMO energy levels. The calculated HOMO and LUMO energy levels are in good agreement with those collected by cyclic voltammetry. The modulation of the fusion positions from [*b*] to [*a*] led to the increased calculated LUMO levels from -3.30 eV (**3**) to -3.16 eV (**4a**), while the calculated HOMO energy levels remain nearly unchanged (-5.15 and -5.14 eV for **3** and **4a**, respectively).

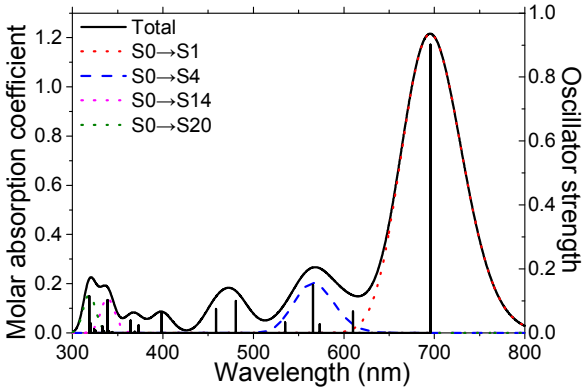

Figure 5. TDDFT predicted absorption spectra of azaBODIPY **4a.** The contributions from the transitions whose strengths are larger than 0.1 have been depicted. The unit for molar absorption coefficient is 10^5 $M^{-1}cm^{-1}$.

In addition, the computed absorption spectra for azaBODIPYs **2**, **3** and **4a** are in

agreement with the experimental ones, with the absorption maximum for all these dyes mainly contributed from the HOMO to the LUMO transition (Table S6 in the supporting information). The TDDFT predicted absorption spectra of azaBODIPY **4a** (Figure 6) shows an intense peak contributed from S0 → S1 transition with excitation energy of 695 nm and oscillator strength of 0.901. Relatively small still significant absorption peak around 670 nm is mainly from S0 → S4 transition with calculated excitation energy of 565 nm and oscillator strength of 0.150). Similarly, azaBODIPY **3** also has an shoulder peak which is contributed from S0 → S3 transition with calculated excitation energy of 611 nm and oscillator strength of 0.138), along with an intense peak contributed from S0 → S1 transition with excitation energy of 714 nm and oscillator strength of 0.701. Parent azaBODIPY **2** shows a S0 → S1 transition with excitation energy of 646 nm and a S0 → S3 transition with excitation energy of 583 nm. These two excited states both contribute to the maximum absorption of **2**, resulting its broad absorption peak observed from 600-7590 nm (Figure 3a).

Cytotoxicity and bioimaging studies

[*a*]-Fused azaBODIPY **4a** was chosen for biological evaluation in human HEp2 cells and the results are summarized in Figures 6. The biocompatibility of **4a** was evaluated *via* MTT assays. As shown in Figure 6a, there is no evident cell death even at a high concentration of 10 μM **4a**, indicating nontoxicity of the compound to cells under present condition.

AzaBODIPY **4a** was readily taken up by the human HEp2 cells and the images taken by fluorescence microscope were shown in Figure 6. After incubation of HEp2 cells with **4a** for 8 h, this dye proved to be membrane permeable and strong red fluorescence was observed in the cytoplasm (Figure 6c). The fluorescence of **4a** in

cells shows an attractive bright NIR bioimaging property which is potential for further application *in vitro* and *in vivo*.

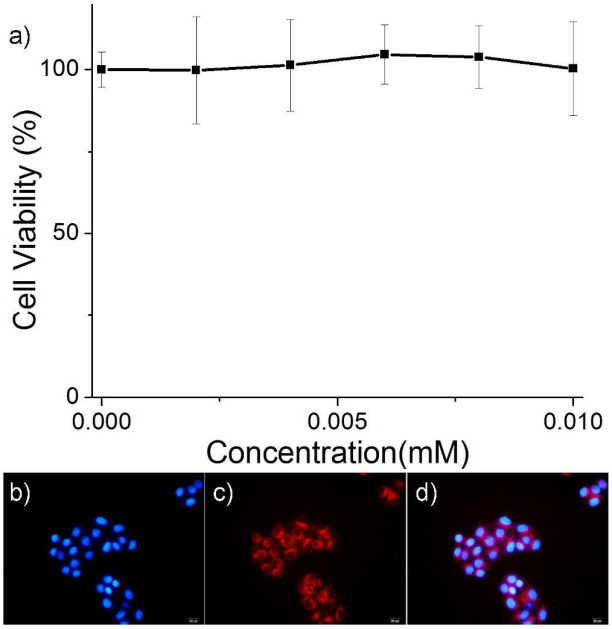

Figure 6. Cell viability of HepG2 cells incubated with **4a** for 24 h (a); fluorescence images of HepG2 cells stained with **4a** (5.0 μM) and DAPI (1.67 μg/ml): (b) DAPI fluorescence, (c) **4a** fluorescence, (d) Merged image (b) and (c); scale bar was 10 uM.

Conclusion

In summary, we have developed a novel method to synthesize unprecedented [*a*]-phenanthrene-fused azaBODIPYs *via* the bromination, Suzuki coupling in concert with the key palladium-catalyzed intramolecular C-H activation reaction on parent azaBODIPY chromophore. The X-ray structures, electronic and optical properties of these π-extended systems were investigated. DFT calculation and cyclic voltammetry studies indicated, in comparison with parent hexaphenylazaBODIPY **2**, the corresponding [*b*]-phenanthrene-fused azaBODIPY **3** showed destabilized HOMO energy levels and stabilized LUMO energy levels, while [*a*]-phenanthrene-fused azaBODIPY **4a** mainly showed destabilized HOMO energy levels. TDDFT

calculation indicated the absorption maximum for all these dyes mainly contributed from the HOMO to the LUMO transition. Compared with corresponding hexaphenylazaBODIPY **2**, [*a*]-phenanthrene-fused azaBODIPYs not only show strong red-shifted NIR absorption, but also have high fluorescent quantum yields. The strong NIR absorption (λ_{abs}^{max} = 745 nm, log ε = 5.1) and fluorescence emission (λ_{em}^{max} = 771 nm, ϕ = 0.35) made [*a*]-phenanthrene-fused azaBODIPY **4a** an attractive bright NIR bioimaging agent.

Experimental Section

General. NMR data were obtained on a 300/500 MHz NMR spectrometer at room temperature. Chemical shifts (δ) are given in ppm relative to TMS. High-resolution mass spectra were obtained using APCI-TOF in positive mode. Absorption and fluorescence emission spectra were recorded on commercial spectrophotometers at room temperature. Relative fluorescence quantum efficiencies of these dyes were obtained by comparing the areas under their emission spectra with that of the reference compound. Non-degassed, spectroscopic grade solvents and a 10 mm quartz cuvette were used. Dilute solutions (0.01<A<0.05) were used to minimize the re-absorption effects. Quantum yields were determined using the following equation[15]:

$$\Phi_x = \Phi_r \times \frac{F_x}{F_r} \times \frac{1-10^{-A_r(\lambda_{ex})}}{1-10^{-A_x(\lambda_{ex})}} \times \frac{n_x^2}{n_r^2}$$

The subscripts *x* and *r* refer respectively to our sample *x* and reference (standard) fluorophore *r* with known quantum yield Φ_r in a specific solvent, *F* stands for the spectrally corrected, integrated fluorescence spectra, $A(\lambda_{ex})$ denotes the absorbance at

the used excitation wavelength λ_{ex}, and *n* represents the refractive index of the solvent (in principle at the average emission wavelength).

Cyclic voltammograms were measured in dichloromethane solution, containing 0.1 M $TBAPF_6$ as the supporting electrolyte, glassy carbon electrode as a working electrode, Pt wire as a counter electrode, and saturated calomel electrode (SCE) as reference electrode at 100 mV s^{-1} of scanning rate at room temperature.

Crystals of azaBODIPYs **2** (CCDC 1445434), **2Br** (CCDC 1445436), **4a** (CCDC 1445439) and 4c (CCDC 1556933) suitable for X-ray analysis were obtained by slow diffusion of anhydrous ethanol into their dichloromethane solutions (within one week period) at room temperature. A suitable crystal was chosen and mounted on a glass fiber using grease. Data were collected using a diffractometer equipped with a graphite crystal monochromator situated in the incident beam for data collection at room temperature. Cell parameters were retrieved using SMART[16] software and refined using SAINT[17] on all observed reflections. The determination of unit cell parameters and data collections were performed with Mo Kα radiation (λ) at 0.71073 Å. Data reduction was performed using the SAINT software, which corrects for Lp and decay. The structure was solved by the direct method using the SHELXS-974 program and refined by least squares method on F^2, SHELXL-97,[18] incorporated in SHELXTL V5.10.[19]

Ground state geometries for azaBODIPYs **1-4** were optimized using Time-Dependent Density Functional Theory (TD-DFT)[20] method at B3LYP/6-31G (d) level[21]. The same method was used for vibrational analysis to verify that the

optimized structures correspond to local minima on the energy surface. TD-DFT computations were used to obtain the vertical excitation energies and oscillator strengths at the optimized ground state equilibrium geometries under the B3LYP/6-31G (d) theoretical level. The geometry optimizations for these dyes in dichloromethane were performed using the Self-Consistent Reaction Field (SCRF) method and Polarizable Continuum Model (PCM). All of the calculations were carried out by the methods implemented in Gaussian 09 package.[22]

Synthesis.

(E)-1-(4-methoxyphenyl)-3-(3,4,5-trimethoxyphenyl)-propenone (S1): Compound **S1** was synthesized from the condensation of 3,4,5-trimethoxybenzaldehyde (1.96 g, 10 mmol) with 4-methoxyacetophenone (1.50 g, 10 mmol) in the presence of KOH (0.8 g, 14 mmol) in anhydrous ethanol (30 mL). The reaction mixture was stirred at room temperature for 30 min. Precipitate was collected, washed with water, and extracted with dichloromethane. Organic layers were combined, and dried over anhydrous Na_2SO_4. Solvent was removed under vacuum to afford compound **S1** as a yellowish green solid in 91% yield (2.98 g). mp 132-133 ^oC. ^1H NMR (300 MHz, $CDCl_3$) δ 8.03 (d, J = 8.7 Hz, 2H), 7.70 (d, J = 15.6 Hz, 1H), 7.41 (d, J = 15.6 Hz, 1H), 6.97 (d, J = 8.7 Hz, 2H), 6.85 (s, 2H), 3.91 (s, 6H), 3.88 (d, J = 4.5 Hz, 3H), 3.87 (s, 3H). ^{13}C NMR ($CDCl_3$, 75 MHz) δ 188.7, 163.4, 153.4, 144.1, 140.1, 130.8, 130.6, 121.2, 113.8, 105.4, 114.0, 61.0, 56.2, 55.5. HRMS (APCI) calcd. for $C_{19}H_{21}O_5$ $[M+H]^+$ 329.1384, found 329.1379.

1-(4-methoxyphenyl)-3-(3,4,5-trimethoxyphenyl)-4-nitro-butan-1-one (S2): To **S1** (3.28 g, 10 mmol) in anhydrous ethanol (30 mL) was added diethylamine (15 mL) and nitromethane (5.4 mL, 0.10 mol). The reaction mixture was heated under reflux for 24 hrs. Solvent was removed under vacuum to give compound **S2** as a white solid in 95% yield (3.70 g). mp 118-119 ^{o}C. ^{1}H NMR (300 MHz, $CDCl_3$) δ 7.90 (d, *J* = 8.7 Hz, 2H), 6.92 (d, *J* = 8.7 Hz, 2H), 6.46 (s, 2H), 4.85-4,79 (m, 1H), 4.70-4.63 (m, 1H), 4.22-4.04 (m, 1H), 3.86 (s, 3H), 3.83 (s, 6H), 3.80 (s, 3H), 3.48-3.14 (m, 1H). ^{13}C NMR ($CDCl_3$, 75 MHz) δ 195.4, 163.8, 153.5, 135.0, 130.3, 130.8, 129.4, 113.9, 104.4, 105.4, 79.5, 60.8, 56.1, 55.5, 41.2, 39.7. HRMS (APCI) calcd. for $C_{20}H_{24}NO_7$ $[M+H]^+$ 390.1547, found 390.1543.

1,7-di(3,4,5-trimethoxylphenyl)-3,5-di(4-methoxylphenyl)azaBODIPY (1): AzaBODIPY **1** was synthesized from the reaction of **S2** (3.89 g, 10 mmol) with $CH_3CO_2NH_4$ (11.6 g, 0.15 mol, 15 equiv) in acetic acid (20 mL) at 120 ^{o}C for 8 h. The reaction mixture was then cooled down to room temperature. The precipitate was filtered, washed with water and dried under vacuum. It was directly applied for the subsequent boron complexation with triethylamine (10 mL, 72 mmol) and $BF_3{\cdot}Et_2O$ (15 mL, 0.14 mol) in toluene. The reaction mixture was stirred at 65 ^{o}C for 0.5 h, diluted with dichloromethane, dried over anhydrous Na_2SO_4, filtered and evaporated under vacuum. The crude product was purified by column chromatography on silica gel (petroleum/ dichloromethane = 3 / 10, v/ v) to give **1** as a red powder in 40% yield (1.47 g). mp > 220 ^{o}C. ^{1}H NMR (300 MHz, $CDCl_3$) δ 8.09 (d, *J* = 8.8 Hz, 4H), 7.19 (s, 4H), 7.01 (d, *J* = 8.7 Hz, 4H), 6.96 (s, 2H), 3.92 (s, 6H), 3.89 (s, 6H), 3.77 (s,

12H). ^{13}C NMR ($CDCl_3$, 75 MHz) δ 161.9, 157.9, 153.2, 145.2, 143.3, 139.2, 128.2, 124.1, 118.5, 114.2, 106.5, 61.0, 56.0, 55.4. HRMS (APCI) calcd. for $C_{40}H_{39}BF_2N_3O_8$ $[M+H]^+$ 738.2793, found 738.2790.

2,6-dibromo-1,7-di(3,4,5-trimethoxylphenyl)-3,5-di(4-methoxylphenyl)azaBODIPY (1Br): 2,6-DibromoazaBODIPY **1Br** was synthesized from dropwise addition of the dichloromethane (10 mL) solution of liquid bromine (370 mg, 2.3 mmol, 2.3 equiv) to **1** (737 mg, 1 mmol) in dry dichloromethane (150 mL). The reaction mixture was stirred at ice-cold condition for 15 min. The crude product was purified by column chromatography on silica gel (petroleum ether/dichloromethane = 1/5, v/v) to give **1Br** as a red powder in 78% yield (697 mg). mp > 220 ^{o}C. ^{1}H NMR (300 MHz, $CDCl_3$) δ 7.75 (d, J = 8.7 Hz, 4H), 7.10 (s, 4H), 6.99 (d, J = 8.7 Hz, 4H), 3.94 (s, 6H), 3.87 (s, 6H), 3.68 (s, 12H). ^{13}C NMR ($CDCl_3$, 75 MHz) δ 161.7, 157.5, 152.6, 144.0, 141.9, 139.3, 132.4, 126.1, 121.7, 113.6, 109.4, 108.2, 61.0, 55.9, 55.3. HRMS (APCI) calcd. for $C_{40}H_{37}BBr_2F_2N_3O_8$ $[M+H]^+$ 894.1004, found 894.0998.

1,7-di(3,4,5-trimethoxylphenyl)-2,6-di(4-t-butylphenyl)-3,5-di(4-methoxylphenyl) azaBODIPY (2): To a dried Schlenk flask were added **1Br** (890 mg 1 mmol), palladium tetrakis(triphenylphosphine) (121 mg, 0.1 mmol), 4-*tert*-butylphenylbronic acid (712 mg, 4 mmol, 4 equiv). This mixture was degassed via three *freeze-pump-thaw* cycles. To the mixture was added dry toluene (10 mL) and the aqueous solution (8 mL) of Na_2CO_3 (0.85 g, 8 mmol) via syringe. The reaction mixture was further degassed *via* three freeze-pump-thaw cycles and purged with argon. The Schlenk flask was sealed and heated to 80 ^{o}C for 12 h, cooled down to

room temperature, washed with brine. Organic layers were combined and dried over anhydrous Na_2SO_4. Solvent was removed under vacuum. The reside was purified via column chromatograph on silica gel (petroleum ether/dichloromethane = 1:4) to afford compound **2** as a red solid in 75% yield (748 mg). mp > 220 ^oC. ^1H NMR (300 MHz, $CDCl_3$) δ 7.46 (d, J = 8.6 Hz, 4H), 7.25 (d, J = 6.9 Hz, 4H), 6.95 (d, J = 8.1 Hz, 4H), 6.78 (d, J = 8.7 Hz, 4H), 6.65 (s, 4H), 3.86 (s, 6H), 3.79 (s, 6H), 3.32 (s, 12H), 1.27 (s, 18H). ^{13}C NMR ($CDCl_3$, 75 MHz) δ 160.8, 158.0, 152.2, 150.3, 145.2, 140.1, 138.0, 133.1, 132.6, 130.6, 130.3, 127.2, 125.4, 122.9, 113.3, 108.3, 60.9, 55.3, 55.2, 34.6, 31.3. HRMS (APCI) calcd. for $C_{60}H_{63}BF_2N_3O_8$ $[M+H]^+$ 1002.4671, found 1002.4663.

[*b*]-Fused azaBODIPY 3: To **2** (50 mg, 0.05 mmol) in dichloromethane (30 mL) was dropwise added $FeCl_3$ (84 mg, 0.5 mmol) in CH_3NO_2 (2 mL) *via* syringe. The reaction mixture was stirred for 5 min and was quenched by adding water (50 mL). The mixture was extracted with CH_2Cl_2. Organic layers were combined and dried over anhydrous Na_2SO_4. Solvent was removed under vacuum to afford **3** as a red solid in 87% yield (43 mg).mp > 220 ^oC. ^1H NMR (300 MHz ,$CDCl_3$) δ 9.47 (d, J = 6.0 Hz, 2H), 8.35 (s, 2H), 8.06 (d, J = 9.0 Hz, 2H), 7.99 (s, 2H), 7.38 (d, J = 9.0 Hz, 4H), 6.78 (s, 4H), 4.10 (s, 6H), 4.02 (s, 6H), 3.65 (s, 12H), 1.43 (s, 18H). ^{13}C NMR (75 MHz, $CDCl_3$) δ 162.2, 152.7, 150.7, 150.1, 148.7, 138.3, 138.1, 137.8, 132.4, 128.5, 128.3, 126.7, 125.7, 125.5, 125.3, 120.0, 117.5, 114.5, 108.9, 108.4, 61.0, 56.1, 55.7, 35.1, 31.3. HRMS (APCI) calcd. for $C_{60}H_{59}BF_2N_3O_8$ $[M+H]^+$ 998.4358, found 998.4348.

1,7-di(2-bromo-3,4,5-trimethoxylphenyl)-2,6-di(4-t-butylphenyl)-3,5-di(4-methoxylphenyl)azaBODIPY (2Br): To **2** (200 mg, 0.2 mmol) in dried dichloromethane (100 mL) was dropwisely added liquid bromine (639 mg, 4.0 mmol, 20 equiv) in dried dichloromethane (10 mL). The reaction mixture was stirred at ice-cold condition for 5 min. The crude product was purified by column chromatography on silica gel (petroleum ether : dichloromethane = 1:1) to give **2Br** as a red powder in 82% yield (223 mg). mp > 220 ^{o}C. ^{1}H NMR (500 MHz, $CDCl_3$) δ 9.62 (s, 2 H), 9.08 (s, 2H), 7.20 (d, J = 8.4 Hz, 4H), 7.41-7.33 (m, 4H), 7.05 (d, J = 8.7 Hz, 4H), 4.13 (s, 6H), 4.04 (s, 6H), 3.99 (s, 6H), 3.92 (s, 6H), 1.42 (s, 18H). ^{13}C NMR (126 MHZ, $CDCl_3$) δ 161.1, 158.2, 152.2, 150.9, 150.1, 144.9, 143.0, 140.9, 135.3, 132.6, 129.9, 129.5, 129.1, 124.8, 123.2, 113.4, 111.8, 110.8, 61.1, 60.8, 56.3, 55.2, 34.5, 31.2. HRMS (APCI) Calcd. for $C_{60}H_{61}O_8N_3BBr_2F_2$ $[M+H]^+$ 1160.2861 found 1160.2859.

[*a*]-Fused azaBODIPY 4a: To **2Br** (58 mg, 0.05 mmol) in toluene (5 mL) was added $Pd(OAc)_2$ (3.4 mg, 0.015 mmol), PPh_3 (8.0 mg, 0.03 mmol) and K_2CO_3 (21 mg, 0.15 mmol, 3 equiv). The resulting suspension was stirred at 120 ^{o}C for 32 h under argon. The crude product was purified by column chromatography on silica gel (petroleum ether/ dichloromethane = 1/1, v/v) to give **4a** as a blue chip powder in 46% yield (27 mg). mp > 220 ^{o}C. ^{1}H NMR (300 MHz, $CDCl_3$) δ 7.52 (d, J = 8.5 Hz, 4H), 7.06 (d, J = 3.0 Hz, 4H), 6.82 (d, J = 9.0 Hz, 4H), 6.73 (d, J = 8.5 Hz, 4H), 6.45 (s, 2H), 3.85 (s, 6H), 3.82 (s, 12H), 3.72 (s, 6H), 1.22 (s, 18H). ^{13}C NMR (126 MHz, $CDCl_3$) δ 160.9, 156.1, 153.7, 152.8, 149.2, 145.5, 141.8, 131.3, 130.3, 125.6, 125.5, 125.0, 124. 8,

124.4, 124.2, 123.1, 122.5, 114.1, 106.6, 61.6, 60.5, 57.1, 55.3, 35.2, 31.5. HRMS (APCI) Calcd. for $C_{60}H_{59}O_8N_3BF_2$ $[M+H]^+$ 998.4358 found 998.4350.

(E)-1-(4-methoxyphenyl)-3-(2-bromophenyl)-propenone (S3) was obtained as a yellow solid from 2-bromobenzaldehyde (1.85 g, 10 mmol) and 4-methoxyacetophenone (1.50 g, 10 mmol) following the same procedure as **S1** in 84% yield (2.65 g). mp 75-76 ^oC. ^1H-NMR (300 MHz, $CDCl_3$) δ 8.14 (d, J = 15.0 Hz, 1H), 8.05 (d, J = 8.3 Hz, 2H), 7.74 (d, J = 8.3 Hz, 1H), 7.64 (d, J = 8.3 Hz, 1H), 7.47 - 7.34 (m, 2H), 7.25 - 7.01 (m, 1H), 7.00 (d, J = 8.3 Hz, 2H), 3.90 (s, 3H). ^{13}C-NMR (75 MHz, $CDCl_3$) δ 188.6, 163.5, 142.4, 135.3, 133.5, 131.1, 131.0, 130.1, 127.9, 127.7, 125.8, 125.0, 113.8, 55.5. HRMS (APCI) calcd. for $C_{16}H_{13}BrO_2$ $[M+H]^+$: 317.0172, found 317.0170.

1-(4-methoxyphenyl)-3-(2-bromophenyl)-4-nitro-butan-1-one (S4) was obtained as a yellow oil from **S3** (3.17 g, 10 mmol) following the same procedure as **S2** in 90% yield (3.4 g). ^1H NMR (300 MHz, $CDCl_3$) δ 7.91 (d, J = 9.0 Hz, 2H), 7.58 (d, J = 8.0 Hz, 1H), 7.27 - 7.25 (m, 2H), 7.14 - 7.11 (m, 1H), 6.91 (d, J = 9.1 Hz, 2H), 4.86 - 4.83 (m, 2H), 4.69 - 4.64 (m, 1H), 3.85 (s, 3H), 3.46 (d, J = 7.3 Hz, 2H). ^{13}C NMR (75 MHz, $CDCl_3$) δ: 195.2, 163.9, 138.0, 133.8, 130.4, 129.3, 129.2, 128.1, 128.0, 124.5, 113.9, 77.7, 55.6, 39.7, 38.3. HRMS (APCI) calcd. for $C_{17}H_{17}BrNO_4$ $[M+H]^+$ 378.0336, found 378.0334.

1,7-di(2-bromophenyl)-3,5-di(4-methoxylphenyl)azaBODIPY (5) was obtained as a gray solid from **S4** (3.77 g, 10 mmol) following the same procedure as **1** in 39% yield (1.29 g). mp > 220 ^oC. ^1H-NMR (300 MHz, $CDCl_3$) δ: 8.06 (d, J = 8.3 Hz, 4H),

7.60 (d, *J* = 7.3 Hz, 4H), 7.26 – 7.20 (m, 4H), 7.14 (d, *J* = 8.4 Hz, 2H), 6.97 (d, *J* = 8.5 Hz, 4H), 3.84 (s, 6H). ^{13}C-NMR (75 MHz, $CDCl_3$) δ 162.1, 157.6, 146.0, 142.2, 133.8, 133.5, 132.7, 131.9, 129.7, 126.7, 123.9, 123.3, 114.4, 55.5. HRMS (APCI) calcd. for $C_{34}H_{25}BF_2Br_2N_3O_2$ $[M+H]^+$ 715.0402, found 715.0383.

1,7-di(2-(4-t-butylphenyl)-phenyl)-3,5-di(4-methoxylphenyl)azaBODIPY (6) was obtained from **5** (185 mg, 0.26 mmol) and 4-*tert*-butylphenylbronic acid (153 mg, 1.04 mmol) following the same procedure as **2** in 92% yield (196 mg). mp > 220 ^{o}C. ^{1}H NMR (500 MHz, $CDCl_3$) δ 8.02 (d, *J* = 7.3 Hz, 2H), 7.61 (d, *J* = 8.8 Hz, 4H), 7.46 - 7.40 (m, 10H), 7.25 (d, *J* = 9.7 Hz, 4H), 6.83 (d, *J* = 8.9 Hz, 4H), 5.87 (s, 2H), 3.83 (s, 6H), 1.38 (s, 18H). ^{13}C NMR (126 MHz, $CDCl_3$) δ 162.0, 157.2, 150.5, 146.4, 143.6, 142.9, 139.4, 133.2, 131.7, 131.4, 130.7, 129.8, 129.1, 127.3, 125.5, 124.7, 123.4, 114.3, 55.7, 35.0, 31.8. HRMS (APCI) Calcd. for $C_{54}H_{51}O_2N_3BF_2$ $[M+H]^+$ 822.4042 found 822.4039.

2,6-dibromo-1,7-di(2-(4-t-butylphenyl)-phenyl)-3,5-di(4-methoxylphenyl)azaBO DIPY (6Br) was obtained from **2e** (205 mg, 0.25 mmol) and liquid bromine (160 mg, 1 mmol) following the same procedure as **2Br** in 72% yield (176 mg). mp > 220 ^{o}C. ^{1}H NMR (300 MHz, $CDCl_3$) δ 7.64 (d, *J* = 8.8 Hz, 2H), 7.58 - 7.51 (m, 4H), 7.50 - 7.37 (m, 6H), 7.20 (d, *J* = 8.3 Hz, 2H), 7.07 (d, *J* = 8.3 Hz, 2H), 6.94 - 6.88 (m, 6H), 6.71 (d, *J* = 8.2 Hz, 2H), 3.83 (s, 6H), 1.26 (s, 18H). ^{13}C NMR (126 MHz, $CDCl_3$) δ 162.0, 157.1, 149.9, 149.5, 145.1, 144.9, 143.4, 143.3, 142.9, 138.8, 132.7, 132.5, 131.8, 130.5, 130.3, 129.8, 129.6, 129.3, 129.2, 126.8, 126.6, 125.3, 125.0, 122.2,

113.9, 55.7, 34.9, 34.8, 31.7, 31.6. HRMS (APCI) Calcd. for $C_{54}H_{49}O_2N_3BBr^{81}BrF_2$ $[M+H]^+$ 980.2227 found 980.2245.

[*a*]-Fused azaBODIPYs 4b and 4c: To a stirred solution of **6Br** (50 mg, 0.05 mmol) in toluene (5 mL) was added $Pd(OAc)_2$ (3.4 mg, 0.015 mmol), PPh_3 (8.0 mg, 0.03 mmol) and Na_2CO_3 (16 mg, 0.15 mmol). The resulting suspension was stirred at 90 ^oC for 8 h under argon. The crude product was purified by column chromatography on silica gel (petroleum ether / dichloromethane = 3/1, v/v) to give **4b** (12 mg, 27 %) and **4c** (19 mg, 38%). **4b**: mp > 220 ^oC. ^1H NMR (300 MHz, $CDCl_3$) δ 9.73 (d, *J* = 7.8 Hz, 2H), 8.60 (d, *J* = 8.2 Hz, 2H), 8.53 (d, *J* = 8.9 Hz, 2H), 7.88 - 7.68 (m, 2H), 7.65 (d, *J* = 8.6 Hz, 2H), 7.58 (d, *J* = 6.9 Hz, 4H), 7.50 (s, 2H), 7.10 (d, *J* = 8.7 Hz, 2H), 3.91 (s, 4H), 1.12 (s, 18H). HRMS (APCI) Calcd. for $C_{54}H_{47}O_2N_3BF_2$ $[M+H]^+$ 818.3724 found 818.3702. **4c**: mp > 220 ^oC. ^1H NMR (300 MHz, $CDCl_3$) δ 9.43 (d, *J* = 7.7 Hz, 1H), 8.59 - 8.52 (m, 2H), 8.17 (d, *J* = 7.5 Hz, 1H), 7.70 - 7.54 (m, 11H), 7.43 (d, *J* = 8.1 Hz, 2H), 7.33 (d, *J* = 8.1 Hz, 2H), 7.15 (d, *J* = 8.5 Hz, 2H), 6.80 (d, *J* = 8.7 Hz, 2H), 5.89 (s, 1H), 3.94 (s, 3H), 3.81 (s, 3H), 1.37 (s, 9H), 1.13 (s, 9H). ^{13}C NMR (126 MHz, $CDCl_3$) δ 161.9, 161.3, 157.3, 157.2, 150.6, 146.0, 143.4, 143.0, 142.8, 139.3, 133.4, 133.2, 131.7, 131.6, 131.4, 131.3, 130.8, 129.9, 129.2, 129.1, 128.9, 128.0, 127.9, 127.7, 127.5, 127.4, 126.6, 125.6, 124.9, 124.6, 123.8, 123.4, 122.7, 120.9, 114.6, 114.3, 55.9, 55.7, 35.0, 31.8, 31.3. HRMS (APCI) Calcd. for $C_{54}H_{49}O_2N_3BF_2$ $[M+H]^+$ 820.3886 found 820.3881.

Cell culture

The HepG2 cancer cells (a human hepatocellular carcinoma cell line) from ATCC

(American Type Culture Collection) were cultured in Dulbecco's Modified Eagle's medium (DMEM, Invitrogen, Carlsbad, CA) with 10 % fetal bovine serum (FBS, ExCell Bio, Shanghai, China) at 37 ℃ with 5 % CO_2.

Cytotoxicity determined by MTT method

The HEp2 cells were plated at 3000 cells per well in a 96-well plate in DMEM medium and allowed to grow for 24 h. A gradient concentration of azaBODIPY **4a** from 2 to 10 μM in fresh medium was added as a replacement and the cells were incubated for 24 h. The working solutions were then removed and the cells were washed with PBS buffer three times. 20 μL MTT (1.5 mg mL^{-1}) was added into each well, and the cells further incubated at 37 ℃ for 4 h in a 10% CO_2 humidified atmosphere. Then the medium was removed and 150 μL DMSO was added. The plate was shaken for 10 minutes and the absorbance was measured at 490 nm using a microplate reader.

Cell incubation and imaging

100, 000 HepG2 cells were seeded into a 6-well plate with the same procedure above. AzaBODIPY **4a** solution in medium (5 μM) was added to the above cells and incubated for another 8 h. The cells were then washed with PBS three times and fixed by 4% formaldehyde for 15 mins. Organelle tracer DAPI (1.67 μg/ml) was added subsequently and incubated for 30 min to stain the nucleus. The above solution in each well was removed and the cells were washed with PBS buffer three times before imaging. After replacement of medium, cells were imaged using a fluorescence microscope with a 20×objective lens.

Supplementary Information (SI) available: Crystal structure data and CIF files, additional photophysical data and spectra, copies of NMR spectra, high resolution mass spectra and additional computational data for all new compounds. This material is available free of charge via the Internet at http://pubs.acs.org.

Acknowledgements

This work is supported by the National Nature Science Foundation of China (21402001, 21372011 and 21672006) and Anhui Province (1508085J07). The calculations have been done on the supercomputing system in the Supercomputing Center of USTC.

Reference:

(1) (a) Chen, H.; Dong, B.; Tang, Y.; Lin, W. *Acc. Chem. Res*. **2017**, *50*, 1410. (b) Pansare, V. J.; Hejazi, S.; Faenza, W. J.; Prud'homme, R. K. *Chem. Mater.* **2012**, *24*, 812. (c) Fischer, G. M.; Daltrozzo, E.; Zumbusch, A. *Angew. Chem. Int. Ed*. **2011**, *50*, 1406. (d) Ong, M. J. H.; Srinivasan, R.; Romieu, A.; Richard, J-A. *Org. Lett*. **2016**, *18*, 5122. (e) Esemoto, N. N.; Yu, Z.; Wiratan, L.; Satraitis, A.; Ptaszek, M. *Org. Lett*. **2016**, *18*, 4590. (f) Lei, Z.; Li, X.; Luo, X.; He, H.; Zheng, J.; Qian, X.; Yang, Y. *Angew. Chem. Int. Ed.* **2017**, *56*, 2979. (g) Cheng, X.; Li, D.; Zhang, Z.; Zhang, H.; Wang, Y. *Org. Lett*. **2014**, *16*, 880. (h) Hiruta, Y.; Koiso, H.; Ozawa, H.; Sata, H.; Hamada, K.; Yabushita, S.; Citterio, D.; Suzuki, K. *Org. Lett*. **2015**, *17*, 3022.

(2) (a) Killoran, J.; Allen, L.; Gallagher, J. F.; Gallagher, W. M.; O'Shea, D. F. *Chem. Commun*. **2002**, 1862. (b) McDonnell, S. O.; Hall, M. J.; Allen, L. T.; Byrne, A.; Gallagher, W. M.; O'Shea, D. F. *J. Am. Chem. Soc.* **2005**, *127*, 16360. (c)

McDonnell, S. O.; O'Shea, D. F. *Org. Lett*. **2006**, *8*, 3493. (d) Murtagh, J.; Frimannsson, D. O.; O'Shea, D. F. *Org. Lett.,* **2009**, *11*, 5386. (e) Wu, D.; O'Shea, D. F. *Org. Lett*. **2013**, *15*, 3392. (f) Ge, Y.; O'Shea, D. F. *Chem. Soc. Rev*. **2016**, *45*, 3846.

(3) (a) Coskun, A.; Yilmaz, M. D.; Akkaya, E. U. *Org. Lett*. **2007**, *9*, 607. (b) Bellier, Q.; Pegaz, S.; Aronica, C.; Guennic, B. L.; Andraud, C.; Maury, O. *Org. Lett.* **2011**, *13*, 22. (c) Gresser, G.; Hartmann, H. M.; Wrackmeyer, K. L.; Riede, M. *Tetrahedron* **2011**, *67*, 7148. (d) Bellier, Q.; Dalier, F.; Jeanneau, E.; Maury, O.; Andraud, C. *New. J. Chem.* **2012**, *36*, 768. (e) Bhuniya, S.; Lee, H.; Jeon, H. M.; Han, J. H.; Lee, J. H.; Park, N.; Maiti, S.; Kang, C.; Kim, J. S. *Chem. Commun.* **2013**, *49*, 7141. (f) Jiao, L.; Wu, Y.; Wang, S.; Hu, X.; Zhang, P.; Yu, C.; Cong, K.; Meng, Q.; Hao, E.; Vicente, M. G. H. *J. Org. Chem*. **2014**, *79*, 1830. (g) Duo, S.; Ma, L.; Zhao, J.; Kucukoz, B.; Karatay, A.; Hayvali, M.; Yaglioglu, H. G.; Elmali, A.; *Chem. Sci*. **2014**, *5*, 489. (h) Ziegler, C. J.; Chanawanno, K.; Hasheminsasab, A.; Zatsikha, Y. V.; Maligaspe, E.; Nemykin, V. N. *Inorg. Chem.* **2014**, *53*, 4751. (i) Jiang, X.; Xi, D.; Sun, C.; Guan, J.; He, M.; Xiao, L. *Tetrahedron Lett*. **2015**, *56*, 4868.

(4) (a) Loudet, A.; Burgess, K. *Chem. Rev.* **2007**, *107*, 4891. (b) Ulrich, G.; Ziessel, R.; Harriman, A. *Angew. Chem., Int. Ed*. **2008**, *47*, 1184. (c) Boens, N.; Leen, V.; Dehaen, W. *Chem. Soc. Rev.* **2012***, 41*, 1130. (d) Lu, H.; Mack, J.; Yang, Y.; Shen, Z. *Chem. Soc. Rev.* **2014**, *43*, 4778. (e) Ni, Y.; Wu, J. *Org. Biomol. Chem*. **2014**, *12*, 3774. (f) Zhao, J.; Xu, K.; Yang, W.; Wang, Z.; Zhong, F. *Chem. Soc. Rev*. **2015**, *44*, 8904.

(5) (a) Zhang, X.; Yu, H.; Xiao, Y. *J. Org. Chem.* **2012**, *77*, 669; (b) Gresser, G.; Hartmann, H. M.; Wrackmeyer, K. L.; Riede, M. *Tetrahedron.* **2011**, *67*, 7148; (c)

Bellier, Q.; Dalier, F.; Jeanneau, E.; Maury, O.; Andraud, C. *New. J. Chem.* **2012**, *36*, 768; (d) Wu, Y.; Cheng, C.; Jiao, L.; Yu, C.; Wang, S.; Wei, Y.; Mu, X.; Hao, E. *Org. Lett*., **2014**, *16*, 748. (e) Daly, H. C.; Sampadro, G.; Bon, C.; Wu, D.; Ismail, G.; Cahill, R. A.; O'shea, D. F. *Eur. J. Med. Chem*. **2017**, *135*, 392.

(6) (a) Jiao, L.; Wu, Y.; Wang, S.; Hu, X.; Zhang, P.; Yu, C.; Cong, K.; Meng, Q.; Hao, E.; Vicente, M. G. H. *J. Org. Chem*. **2014**, *79*, 1830; (b) Bellier, Q.; Pegaz, S.; Aronica, C.; Guennic, B. L.; Andraud, C.; Maury, O. *Org. Lett.* **2011**, *13*, 22.

(7) Loudet, A.; Bandichhor, R.; Burgess, K.; Palma, A.; McDonnell, S. O.; Hall, M. J.; O'Shea, D. F. *Org. Lett*. **2008**, *10*, 4771.

(8) (a) Zhao, W.; Carreira, E. M. *Angew. Chem. Int. Ed*. **2005**, *44*, 1677; (b) Zhao, W.; Carreira, E. M. *Chem. Eur. J.* **2006**, *12*, 725; (c) Jiang, X.; Xi, D.; Sun, C.; Guan, J.; He, M.; Xiao, L. *Tetrahedron Lett*. **2015**, *56*, 4868; (d) Jiang, X.; Xi, D.; Zhao, J.; Yu, H.; Sun, G.; Xiao. L. *RSC Adv*. **2014**, *4*, 60970.

(9) (a) Donyagina, V. F.; Shimizu, S.; Kobayashi, N.; Lukyanets, E. A. *Tetrahedron Lett*. **2008**, *49*, 6152. (b) Lu, H.; Shimizu, S.; Mack, J.; Shen, Z.; Kobayashi, N. *Chem. Asian J.* **2011**, *6*, 1026. (c) Liu, H.; Mack, J.; Fuo, Q.; Lu, H.; Kobayashi, N.; Shen, Z. *Chem. Commun*. **2011**, *47*, 12092. (d) Gresser, G.; Hummert, M.; Hartmann, H.; Leo, K.; Riede, M. *Chem. Eur. J.* **2011**, *17*, 2939. (e) Zhang, W.; Wang, B.; Li, C.; Zhang, J.; Wan, C.; Huang, J.; Liu, J.; Shen, Z.; You, X. *Angew. Chem. Int. Ed*. **2015**, *54*, 9070. (f) Majumdar, P.; Mack, J.; Nyokong, T. *RSC Adv*. **2015**, *5*, 78253.

(10) Zhang, W.; Wang, B.; Li, C.; Zhang, J.; Wan, C.; Huang, J.; Liu, J.; Shen, Z.; You, X. *Angew. Chem. Int. Ed.* **2015**, *54*, 9070.

(11) (a) Descalzo, A. B.; Xu, H.; Xue, Z.; Hoffmann, K.; Shen, Z.; Weller, M. G.; You, X.; Rurack, K. *Org. Lett.* **2008**, *10*, 1581. (b) Jiao, C.; Huang, K.; Wu, J. *Org. Lett.*

2011, *13*, 632. (c) Heyer, E.; Retailleau, P.; Ziessel, R. *Org. Lett*. **2014**, *16*, 2330. (d) Chua, M. H.; Huang, K.; Xu, J.; Wu, J. *Org. Lett.* **2015**, *17*, 4168. (e) Gobo, Y.; Yamamura, M.; Nakamura, T.; Nabeshima, T. *Org. Lett.* **2016**, *18*, 2719.

(12) Sheng, W.; Zheng, Y-Q.; Wu, Q.; Wu, Y.; Yu, C.; Jiao, L.; Hao, E.; Wang, J-Y.; Pei, J. *Org. Lett*. **2017**, *19*, 2893.

(13) (a) Alberico, D.; Scott, M. E.; Lautens, M. *Chem. Rev*. **2007**, *107*, 174. (b) Skonieczny, K.; Gryko, D. T. *J. Org. Chem.* **2015**, *80*, 5753.

(14) (a) Ni, Y.; Zeng, W.; Huang, K.; Wu, J. *Chem. Commun.* **2013**, *49*, 1217. (b) Shimagawa, H.; Mori, H.; Wakamiya, A.; Murata, Y. *Chem. Lett*. **2013**, *42*, 986. (c) Wakamiya, A.; Murakami, T.; Yamaguchi, S. *Chem. Sci.*, **2013**, *4*, 1002.

(15) Lakowicz, J. Principles of Fluorescence Spectroscopy, 3rd ed., Springer-Verlag: New York, **2006**.

(16) Bruker AXS, SMART, Version 5.0, Bruker AXS, Madison, WI. USA. **1998**.

(17) Bruker SAINT V 6.01 (NT), Software for the CCD Detector System, Bruker Analytical X-ray Systems, Madison, WI. **1998**.

(18) Sheldrick, G. M. SHELXL-97, Program for the Refinement of Crystal Structure, University of Gottingen, Germany, **1997**.

(19) Bruker SHELXTL 5.10, Program library for Structure Solution and Molecular Graphics, Bruker Analytical X-ray Systems, Madison, WI. **1998**.

(20) (a) Bauernschmitt, R.; Ahlrichs, *Chem. Phys. Lett*. **1996**, *256*, 454. (b) Casida, M. E. ; C. Jamorski, C.; Casida, K. C., Salahub, D. R. *J. Chem. Phys.***1998**, *108*, 4439. (c) Stratmann, R. E.; Scuseria, G. E.; Frisch, M. J. *J. Chem. Phys*. **1998**, *109*, 8218. (d) Van Caillie C.; Amos, R. D. *Chem. Phys. Lett*. **1999**, *308*, 249. (e) Scalmani, G.; Frisch, M. J.; Mennucci, B.; Tomasi, J.; Cammi, R.; Barone, V. *J. Chem. Phys*. **2006**, *124*, 1.

(21) (a) Becke, A. D. *J. Chem. Phys*. **1993**, *98*, 5648. (b) Lee, C., Yang, W., Parr, R. G. *Phys. Rev. B* **1988**, *37*, 785.

(22) Gaussian 09, Revision D.01, Frisch, M. J.; Trucks, G. W.; et al., Gaussian, Inc., Wallingford CT, **2013**.